Electronic Supplementary Material (ESI) for Polymer Chemistry.
This journal is © The Royal Society of Chemistry 2021

Insights into the co-assemblies formed by different aromatic short-peptides amphiphiles

Cristina Gila-Vilchez,[1] Mari C. Mañas-Torres,[2] Juan A. González-Vera,[3] Francisco Franco-Montalban,[4] Juan A. Tamayo,[4] Francisco Conejero-Lara,[5] Juan Manuel Cuerva,[2] Modesto T. Lopez-Lopez,[1,6] Angel Orte,*[3] and Luis Álvarez de Cienfuegos*[2,6]*

[1] Universidad de Granada, Departamento de Física Aplicada, Facultad de Ciencias, 18071 Granada, Spain

[2] Universidad de Granada, Departamento de Química Orgánica, Facultad de Ciencias, Unidad de Excelencia de Química Aplicada a Biomedicina y Medioambiente (UEQ), 18071 Granada, Spain

[3] Nanoscopy-UGR Laboratory. Dpto de FisicoQuímica, Facultad de Farmacia, UEQ, UGR, 18072-Granada, Spain.

[4] Dpto de Química Farmacéutica y Orgánica, Facultad de Farmacia, (UGR), 18072-Granada, Spain.

[5] Dpto de Química Física, Facultad de Ciencias, UEQ, UGR.

[6] Instituto de Investigación Biosanitaria ibs.GRANADA, Spain.

* Corresponding authors: modesto@ugr.es (M.T. Lopez-Lopez), angelort@ugr.es (Angel Orte), lac@ugr.es (L. Álvarez de Cienfuegos).

SYNTHESIS OF 2-(2-(2-(NAPHTHALEN-2-YLOXY)ACETAMIDO) ACETAMIDO) ACETIC ACID

Ethyl 2-(2-(naphthalen-2-yloxy)acetamido)acetate or ethyl (2-(naphthalen-2-yloxy)acetyl) glycinate. To a stirred solution of 2-(naphthalen-2-yloxy)acetic acid (1.79 g, 8.76 mmol) in chloroform (20 mL) was added N-methylmorpholine (0.95 mL, 8.7 mmol), and isobutyl chloroformate (1.12 mL, 8.7 mmol) at 0 ºC. The solution was stirred at 0 ºC for 5 min. A solution of glycine ethyl ester (1.21 g, 8.7 mmol) and N-methylmorpholine (0.95 mL, 8.7 mmol) in chloroform (20 mL) was added. The solution was allowed to warm to room temperature and stirring for 16 h. The solution was washed with water (2 x 100 mL), dried over magnesium sulfate, and the solvent was removed in vacuo. The crude product was purified by flash column chromatography with ethyl acetate-hexane (1:1) to give ethyl 2-(2(naphthalen-2-yloxy)acetamido)acetate (1.87 g, 75 %). ^{1}H NMR ($CDCl_3$) 7.82-7.19 (m, 8 H), 4.69 (S, 2H), 4.26 (q, 2H), 4.17 (D, 1H), 1.31 (t, 3H) ppm. ^{13}C NMR ($CDCl_3$) 169.5, 168.5, 155.0, 134.3, 129.9, 129.6, 127.7, 127.0, 126.8, 124.4, 118.2, 107.6, 67.3, 61.7, 40.9, 14.15 ppm. HRMS (TOF-ES$^+$): calcd. for $C_{16}H_{18}NO_4$ $[M + H]^+$ 288.1236; found 288.1227.

(2-(2-(Naphthalen-2-yloxy)acetamido)acetic acid or (2-(naphthalen-2-yloxy)acetyl)-glycine. Ethyl 2-(2-(naphthalen-2-yloxy)acetamido)acetate (975 mg, 3.40 mmol) was dissolved in 30 mL of THF-H_2O (3:1). Lithium hydroxide (0.43 g) was added and the solution was stirred for 16 h. Water (100 mL) was added, and then hydrochloric acid (1.0 M) was added dropwise until the pH was lowered to pH 3. The resulting white precipitate was collected by filtration and washed with water and hexane before being dried in vacuo to give 2-(2-(naphthalen-2-yloxy)acetamido)acetic acid as a white solid (500 mg, 57 %). ^{1}H NMR (DMSO) 12.7 (s, 1H), 8.48 (t, 1H), 7.86-7.24 (m, 7H), 4.65 (s, 2H), 3.83 (d, 2H) ppm. ^{13}C NMR (DMSO) 171.5, 168.5, 155.9, 134.5, 129.8, 129.2, 128.0, 127.2, 126.9, 124.3, 120.0, 117.9, 67.32. MS (TOF-ES$^-$): calcd. for $C_{14}H_{12}NO_4$ $[M - H]^-$ 258.0766; found 258.0758.

Ethyl 2-(-2-(2-(naphthalen-2-yloxy)acetamido)acetamido)acetate or ethyl (2-(naphthalen-2-yloxy)acetyl)-glycyl-glycinate. To a stirred solution of 2-(2-(naphthalen-2-yloxy)acetamido)acetic acid (350 mg, 1.28 mmol) in chloroform (12 mL) was added N-methylmorpholine (142 µL, 1.28 mmol), and isobutyl chloroformate (166 µL, 1.28 mmol) at 0 ºC. The solution was stirred at 0 ºC for 5 min. A solution of glycine ethyl ester (178 mg, 1.28 mmol)

and N-methylmorpholine (142 μL, 1.28 mmol) in chloroform (12 mL) was added. The solution was allowed to warm to room temperature and stirring for 12 h. The solution was washed with water (2 x 30 mL), dried over magnesium sulfate, and the solvent was removed in vacuo. The crude product was purified by flash column chromatography, eluting ethyl acetate-hexane (3:1) to give ethyl 2-(2-(2-(naphthalen-2-yloxy)acetamido)acetamido)acetate (383 mg, 83 %). ^{1}H NMR ($CDCl_3$) 7.79-7.14 (m, 8H), 6.68 (bt, 1H), 4.66 (s, 2H), 4.20 (q, 2H), 4.11 (d, 2H), 4.0 (d, 2H), 1.27 (t, 3H) ppm. 13C NMR (CDCl3) 169.5, 168.9, 168.6, 154.9, 134.2, 130.0, 129.5, 127.7, 126.9, 126.7, 124.4, 118.2, 107.4, 67.1, 42.5, 41.3, 14.1 ppm. MS (TOF-ES$^+$): calcd. for $C_{18}H_{20}N_2O_5Na$ $[M + Na]^+$ 367.1270; found 367.1294.

2-(2-(2-(naphthalen-2-yloxy)acetamido)acetamido)acetic acid or (2-(naphthalen-2-yloxy)acetyl)-glycyl-glicine. Ethyl 2-(2-(2-(naphthalen-2-yloxy)acetamido) acetamido) acetate (200 mg, 0.56 mmol) was dissolved in 10 mL of THF-H_2O (3:1). Lithium hydroxide (70 mg) was added and the solution was stirred for 16 h. Water (50 mL) was added, and then hydrochloric acid (1.0 M) was added dropwise until the pH was lowered to pH 3. The resulting white precipitate was collected by filtration and washed with water and hexane before being dried in vacuo to give 2-(2-(2-(naphthalen-2-yloxy)acetamido)acetamido)acetic acid as a white solid (137 mg, 74 %).^{1}H NMR (DMSO) 12.58 (s, 1H), 8.41 (t, 1H), 8.24 (t, 1H), 7.88-7.27 (m, 7H), 4.67 (s, 2H), 3.84 (d, 2H), 3.78 (d, 2H) ppm. ^{13}C NMR (DMSO) 171.6, 169.4, 168.3, 156.0, 134.5, 129.8, 129.2, 128.0, 127.2, 126.9, 124.3, 119.0, 107.8, 107.8, 67.4, 42.0, 41.0 ppm. MS (TOF-ES+) calcd. for $C_{16}H_{17}N_2O_5$ $[M + H]^+$ 317.1137; found 317.1120.

SYNTHESIS OF 2-(-2-(2-(NAPHTHALEN-2-YLOXY)ACETAMIDO) PROPANAMIDO)PROPANOIC ACID or N-[2-(2-NAPHTHALENYLOXY) ACETYL]-L-ALANYL-L-ALANINE

tert-Butyl 2-(Naphthalen-2-yloxy)acetate. To a stirred solution of 2-naphthol (322 mg, 2.24 mmol), and potassium carbonate (1.55 g, 11.2 mmol, 5 eq) in toluene (15 mL) was added chloro-tert-butyl acetate (0.352 mL, 2.46 mmol, 1.1 eq). The solution was heated at 70 ºC for 4 h. Chloroform (30 mL) was added , and the solution was washed with water (4 x 20 mL). The organic phase was dried with magnesium sulfate and the solvent removed in vacuo. The crude product was purified by flash column chromatography, eluting 10 % ethyl acetate in hexane, to give tert-butyl 2-(naphthalen-2-yloxy)acetate (479 mg, 83 %) as a white solid. ^{1}H NMR ($CDCl_3$): 7.80-7.10 (m, 7H), 4.66 (s, 3H), 1.54 (s, 9 H). ^{13}C NMR ($CDCl_3$) 168.0, 155.9, 134.3, 129.7, 129.4, 127.7, 126.9,

126.5, 124.0, 118.7, 107.1, 82.5, 65.8, 28.1 ppm. MS (TOF-ES$^+$): calcd. for $C_{16}H_{19}O_3$ $[M + H]^+$ 259.1334; found 259.1337.

2-(Naphthalen-2-yloxy)acetic acid. tert-butyl 2-(Naphthalen-2-yloxy)acetate (200 mg, 0.77 mmol) was dissolved in chloroform (10 mL). Trifluoroacetic acid (0.32 mL, 3.57 mmol) was added and the solution was stirred for 20 h. Hexane (40 mL) was added, and the resulting white precipitate was collected, washed with hexane and dried to afford 2-(naphthalen-2-yloxy)acetic acid as a white solid (140 mg, 90 %). ^{1}H NMR (CD_3OD): 7.77-7.19 (m, 7 H), 4.81 (s, 2H) ppm. ^{13}C NMR (CD_3OD) 171.2, 155.9, 129.2, 129.1, 127.2, 126.1, 123.6, 118.1, 64.6 ppm. HRMS (TOF-ES$^+$): calcd. for $C_{12}H_{11}O_3$ $[M + H]^+$ 203.0708; found 203.0706.

Ethyl 2-(2-(naphthalen-2-yloxy)acetamido)propanoate or ethyl (2-(naphthalen-2-yloxy)acetyl)-L-alaninate. To a stirred solution of 2-(naphthalen-2-yloxy)acetic acid (202 mg, 1.0 mmol) in chloroform (6 mL) was added N-methylmorpholine (0.11 mL, 1 mmol), and isobutyl chloroformate (0.13 mL, 1.0 mmol) at 0 ºC. The solution was stirred at 0 ºC for 5 min. A solution of alanine ethyl ester (153 mg, 1 mmol) and N-methylmorpholine (0.11 mL, 1.0 mmol) in chloroform (6 mL) was added. The solution was allowed to warm to room temperature and stirring for 12 h. The solution was washed with water (2 x 30 mL), dried over magnesium sulfate, and the solvent was removed in vacuo. The crude product was purified by flash column chromatography, eluting ethyl acetate-hexane (1:3) to give ethyl 2-(2(naphthalen-2-yloxy)acetamido)propanoate (200 mg, 66 %). ^{1}H NMR ($CDCl_3$) 7.83-7.19 (m, 7 H), 4.72 (m, 1H), 4.66 (s, 2H), 4.24 (q, 2H), 1.50 (d, 3H), 1.30 (t, 3H) ppm. ^{13}C NMR ($CDCl_3$) 172.5, 167.8, 155.0, 134.3, 129.9, 129.5, 127.7, 127.0, 126.7, 124.4, 118.2, 107.7, 67.3, 61.7, 47.8, 18.4, 14.1 ppm. HRMS (TOF-ES$^+$): calcd. for $C_{17}H_{20}NO_4$ $[M + H]^+$ 302.1392; found 302.1404.

(2-(2-(Naphthalen-2-yloxy)acetamido)propanoic acid or (2-(naphthalen-2-yloxy)acetyl)-L-alanine. Ethyl 2-(2(naphthalen-2-yloxy) acetamido)propanoate (800 mg, 2.65 mmol) was dissolved in 30 mL of THF-H_2O (3:1). Lithium hydroxide (0.3 g) was added and the solution was stirred for 16 h. Water (100 mL) was added, and then hydrochloric acid (1.0 M) was added dropwise until the pH was lowered to pH 3. The resulting white precipitate was collected by filtration and washed well with water and hexane before being dried in vacuo to give 2-(2-(naphthalen-2-yloxy)acetamido) propanoic acid as a white solid (670 mg, 92 %). ^{1}H NMR (DMSO) 12.7 (s, 1H), 8.45 (s, 1H), 7.87-7.26 (m, 7H), 4.66 (d, 2H), 4.35 (m, 1H), 1.35 (d, 3H) ppm. ^{13}C NMR (DMSO) 174.3, 167.8, 156.1, 134.5, 129.8, 129.2, 128.0, 127.2, 126.9, 124.3,

119.1, 107.9, 67.2, 47.7, 17.6 ppm. MS (TOF-ES$^-$): calcd. for $C_{15}H_{14}NO_4$ $[M - H]^-$ 272.0923; found 272.0932.

Ethyl 2-(-2-(2-(naphthalen-2-yloxy)acetamido)propanamido)propanoate or ethyl (2-(naphthalen-2-yloxy)acetyl)-L-alanyl-L-alaninate. To a stirred solution of (2-(2-(Naphthalen-2-yloxy)acetamido)propanoic acid (136 mg, 0.5 mmol) in chloroform (5 mL) was added N-methylmorpholine (0.55 μL, 0.5 mmol), and isobutyl chloroformate (64 μL, 0.5 mmol) at 0 ºC. The solution was stirred at 0 ºC for 5 min. A solution of L-alanine ethyl ester (77 mg, 0.5 mmol) and N-methylmorpholine (0.55 μL, 0.5 mmol) in chloroform (5 mL) was added. The solution was allowed to warm to room temperature and stirring for 12 h. The solution was washed with water (2 x 30 mL), dried over magnesium sulfate, and the solvent was removed in vacuo. The crude product was purified by flash column chromatography, eluting ethyl acetate-hexane (2:1) to give ethyl 2-(-2-(2-(naphthalen-2-yloxy)acetamido)propanamido)propanoate (113 mg, 61 %). ^{1}H NMR ($CDCl_3$) 7.83-7.18 (m, 7H), 6.62 (d, 1H), 4.69-4.63 (m, 3H), 4.55 (m, 1H), 4.23 (q, 2H), 1.49 (d, 3H), 1.42 (d, 3H), 1.30 (t, 3H) ppm. ^{13}C NMR ($CDCl_3$) 172.6, 171.2, 168.0, 155.0, 134.0, 130.0, 129.5, 127.7, 127.0, 126.7, 124.4, 118.2, 107.5, 67.2, 61.6, 48.4, 48.3, 18.5, 18.2, 14.1 ppm. MS (TOF-ES$^+$): calcd. for $C_{20}H_{25}N_2O_5$ $[M + H]^+$ 373.1763; found 373.1764.

2-(-2-(2-(Naphthalen-2-yloxy)acetamido)propanamido)propanoic acid, or N-[2-(2-Naphthalenyloxy)acetyl]-L-alanyl-L-alanine. Ethyl 2-(-2-(2-(naphthalen-2-yloxy)acetamido)propanamido)propanoate (215 mg, 0.58 mmol) was dissolved in 20 mL of THF-H_2O (3:1). Lithium hydroxide (72 mg) was added and the solution was stirred for 16 h. Water (500 mL) was added, and then hydrochloric acid (1.0 M) was added dropwise until the pH was lowered to pH 3. The resulting white precipitate was collected by filtration and washed with water and hexane before being dried in vacuo to give 2-(-2-(2-(Naphthalen-2-yloxy)acetamido)propanamido)propanoic acid as a white solid (139 mg, 70 %). ^{1}H NMR (CD_3OD) 7.82-7.28 (m, 7H), 4.69 (s, 2H), 4.57 (q, 1H), 4.40 (q, 1H), 1.45 (d, 3H), 1.39 (d, 3H) ppm. ^{13}C NMR (CD_3OD) 174.5, 172.8, 169.2, 155.5, 134.5, 129.3, 127.2, 126.6, 126.1, 123.7, 118.1, 107.1, 66.7, 48.4, 47.8, 17.1, 16.2 ppm. MS (TOF-ES$^+$) calcd. for $C_{18}H_{20}N_2O_5Na$ $[M + Na]^+$ 367.1270; found 367.1290.

SYNTHESIS OF 2-(-2-(2-(NAPHTHALEN-2-YLOXY)ACETAMIDO) PROPANAMIDO)PROPANOIC ACID or N-[2-(2-NAPHTHALENYLOXY) ACETYL]-D-ALANYL-D-ALANINE

The same protocol described above was used to obtain the following yields:

Ethyl (2-(naphthalen-2-yloxy)acetyl)-D-alaninate (78 %)

2-(Naphthalen-2-yloxy)acetyl-D-alanine (77 %)

Ethyl (2-(naphthalen-2-yloxy)acetyl)-D-alanyl-D-alaninate (43 %)

N-[2-(2-Naphthalenyloxy)acetyl]-D-alanyl-D-alanine (55 %)

Copies of ^{1}H NMR and ^{13}C NMR of Nap-AA (L and D enantiomers report same spectra)

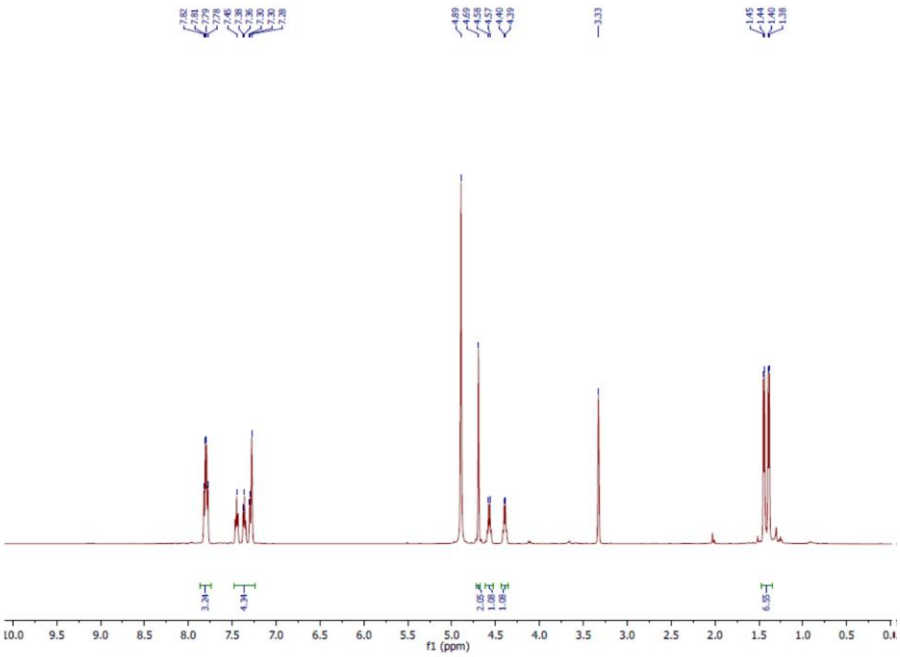

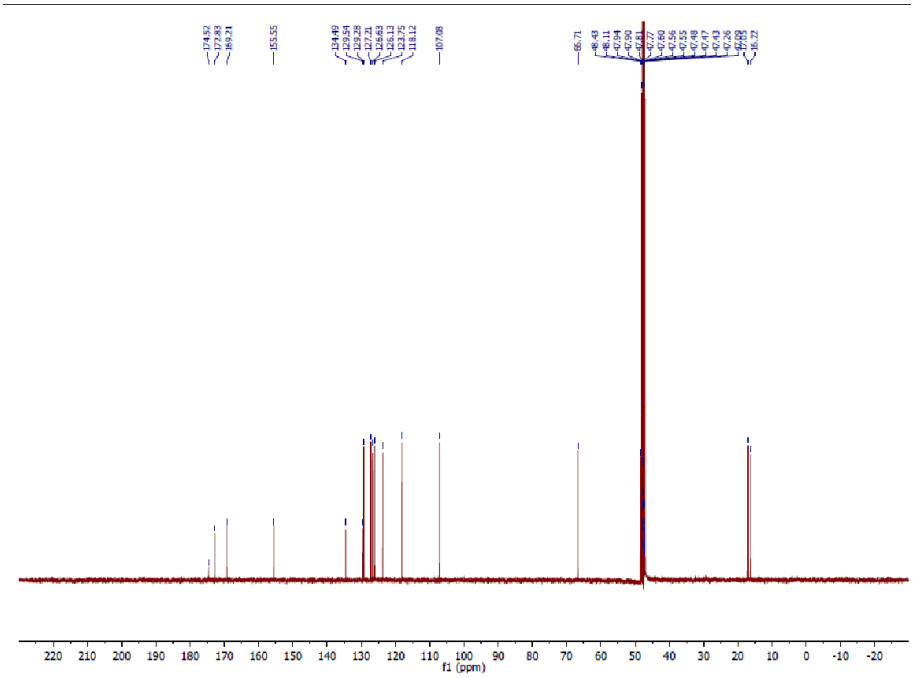

Copies of ^{1}H NMR and ^{13}C NMR of Nap-GG

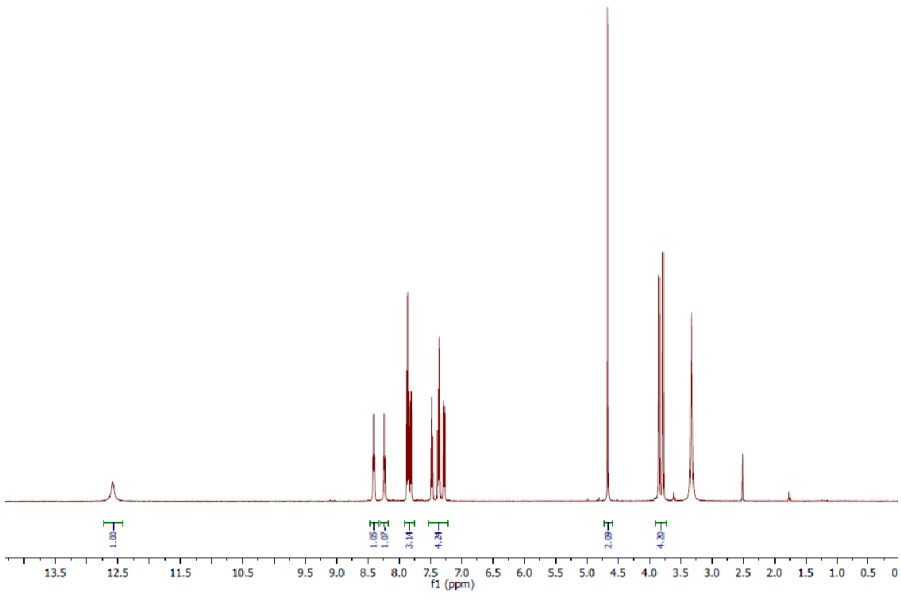

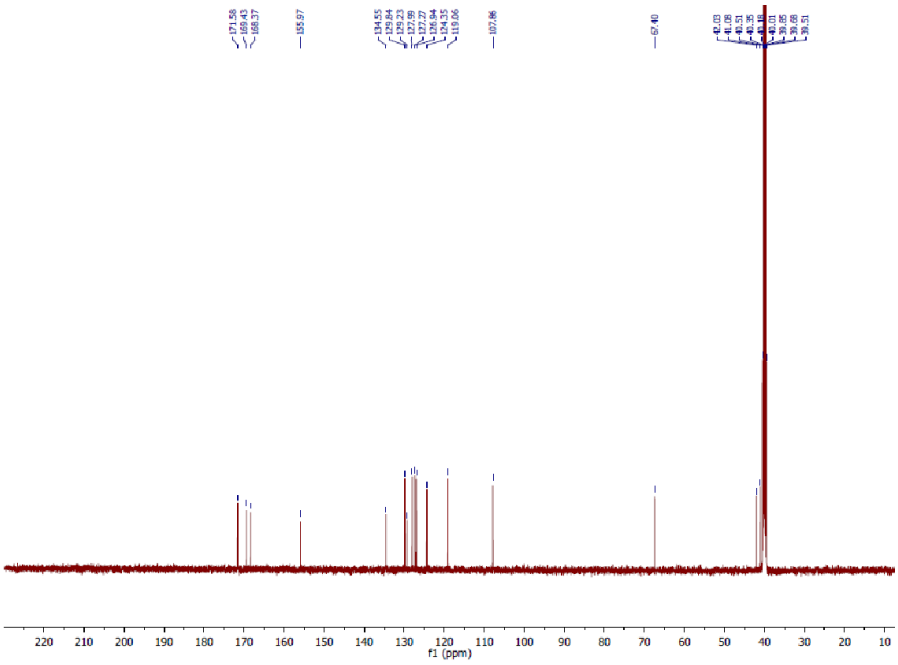
171.58
169.43
168.37
155.97
134.55
129.64
129.32
127.99
127.77
126.84
124.35
119.04
107.86
67.40
42.03
41.08
40.51
40.35
40.18
40.01
39.85
39.68
39.51
220 210 200 190 180 170 160 150 140 130 120 110 100 90 80 70 60 50 40 30 20 10
f1 (ppm)

FIGURES

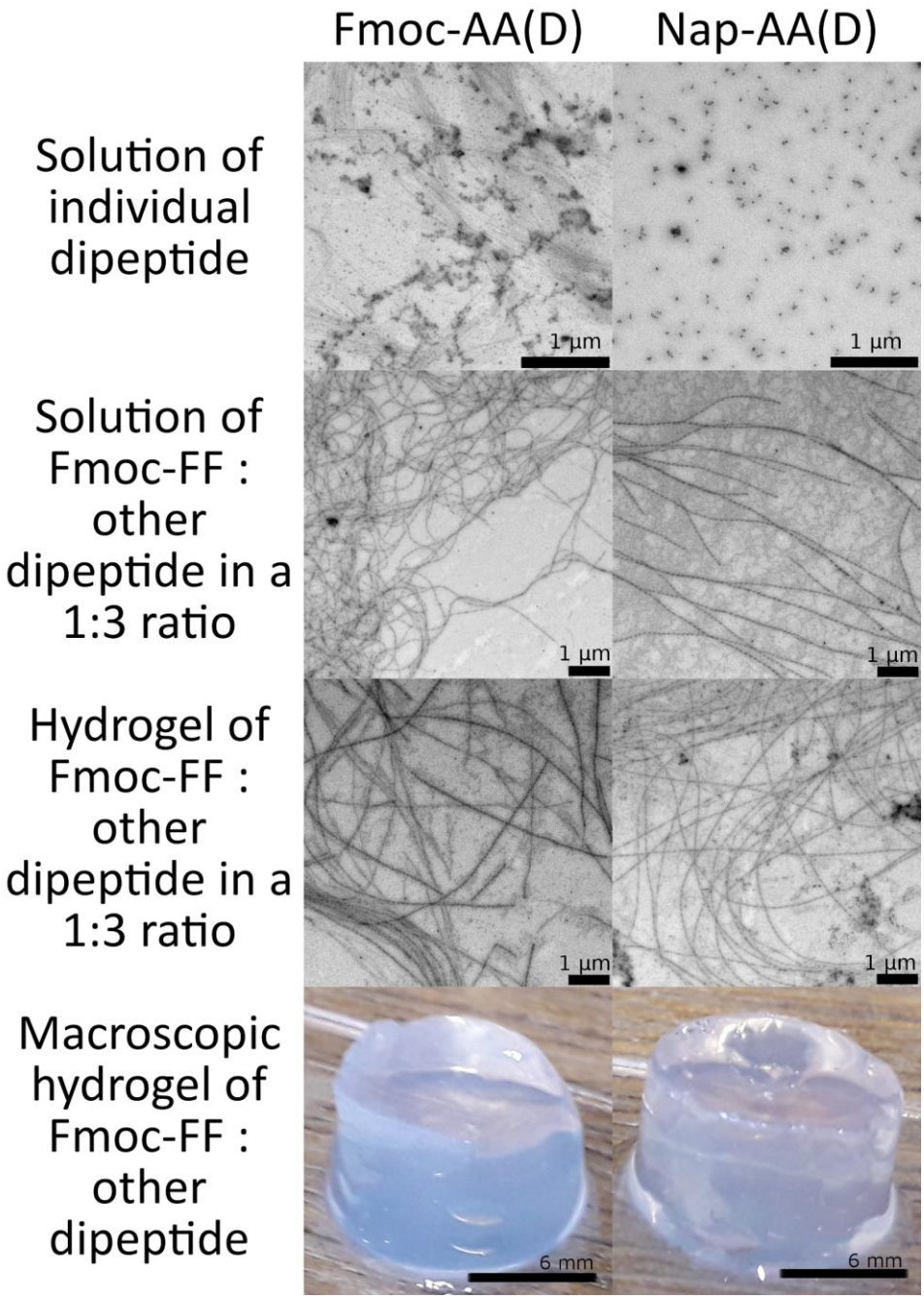

Figure S1. TEM images of 10 mM samples diluted in water at 1:5 proportion of (A), (B) sodium salt solution of each one of individual dipeptides. Sodium salt solution of Fmoc-FF and: Fmoc-AA(D) (C) and Nap-AA(D) (D) at 1:3 proportion without δ-gluconolactone. Hydrogels, formed by the addition of δ-gluconolactone, of Fmoc-FF and: Fmoc-AA(D) (E) and Nap-AA(D) (F) at 1:3 proportion; and macroscopic images of hydrogels formed by Fmoc-FF and: Fmoc-AA(D) (G) and Nap-AA(D) (H) at a final concentration of 10 mM.

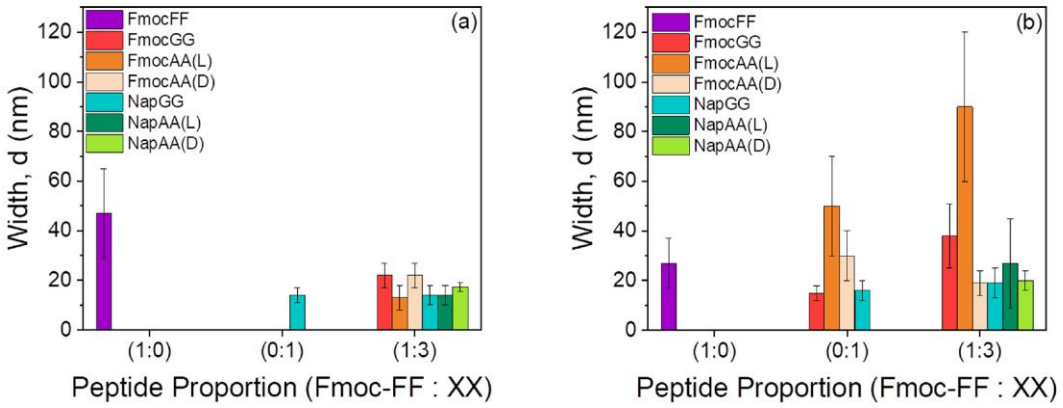

Figure S2. Width of peptides fibers measured from TEM images of (a) peptides in solution and (b) peptide hydrogels.

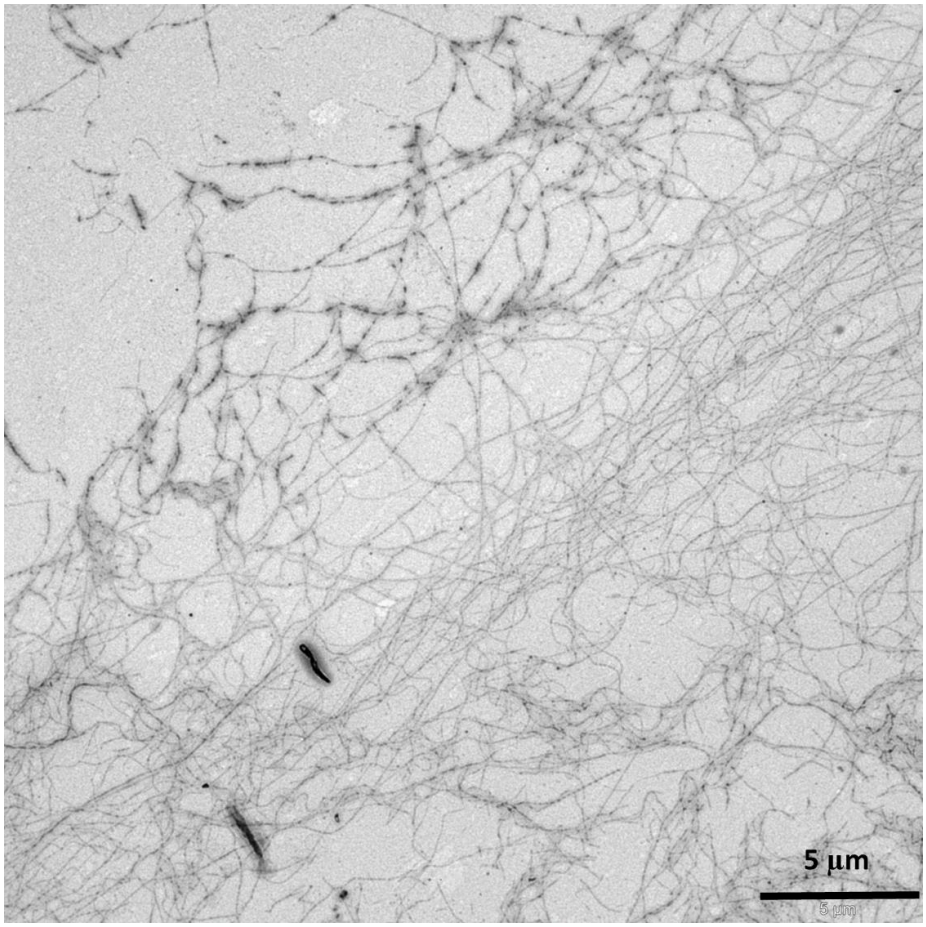

Figure S3. TEM images of Fmoc-FF:Fmoc-GG solutions at 1:3 (0.5 mM:1.5 mM) proportion. Image shows the formation of fibrils by multiple aggregation of nanospheres.

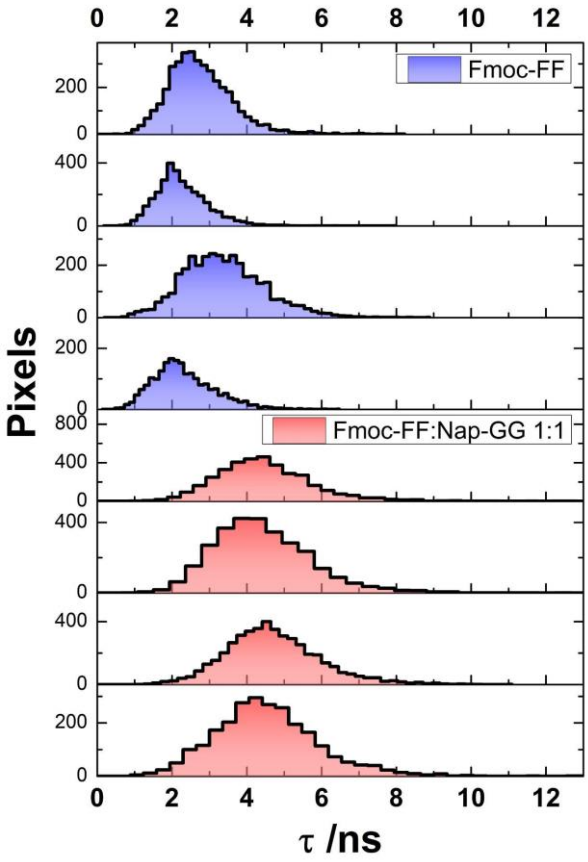

Figure S4. Fluorescence lifetime distributions of AQui (12.5 μM) interacting with hydrogels fibers of individual dipeptide Fmoc-FF (blue distributions) and those formed by Fmoc-FF and Nap-GG at 1:1 (5 mM:5 mM) proportion.

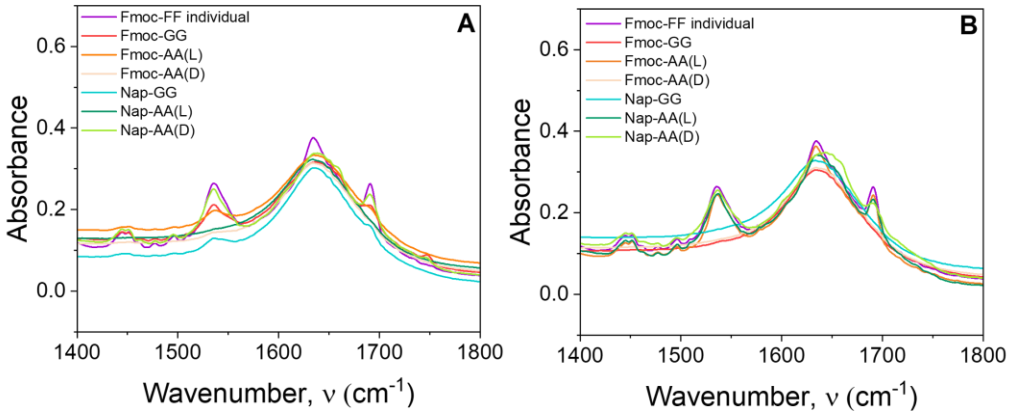

Figure S5. FTIR transmittance as a function of the wavenumber for hydrogels of individual dipeptide Fmoc-FF and those formed by Fmoc-FF and other dipeptides at (A) 1:1 (5 mM:5 mM) and (B) 1:3 (2.5 mM:7.5 mM) proportion.

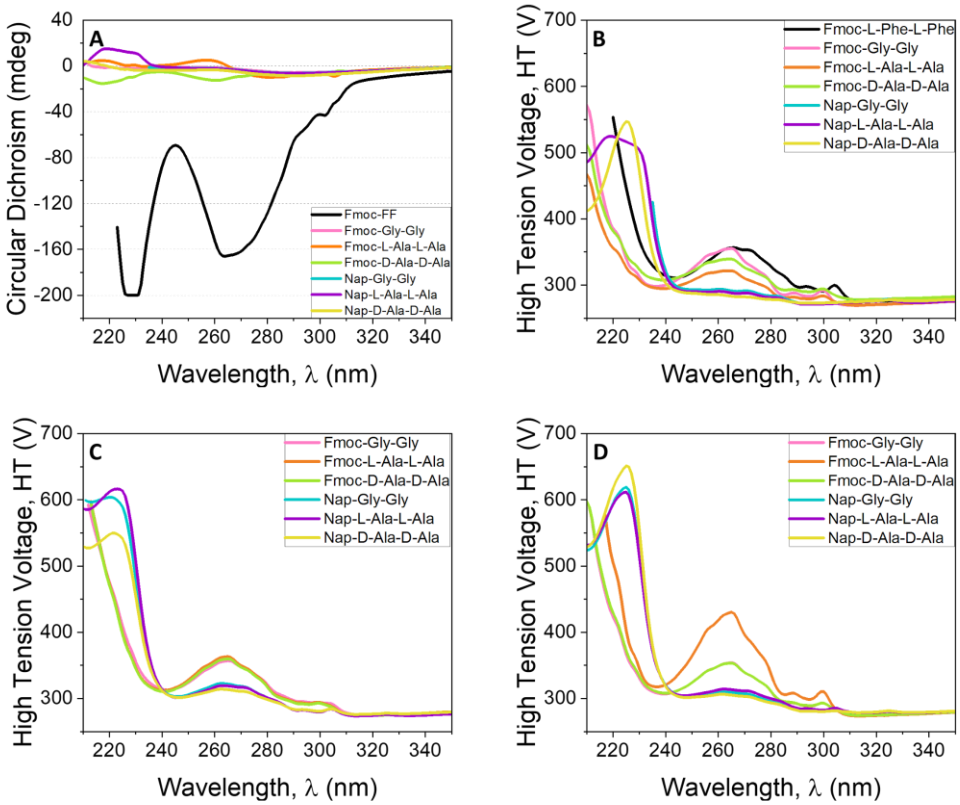

Figure S6. CD spectra for hydrogels formed by individual dipeptides (10 mM) (A). HT spectra for individual dipeptides (B) and for mixtures of Fmoc-FF: other dipeptides at 1:1 (2.5 mM: 2.5 mM) proportion (C) and at 1:3 (1.25 mM: 3.75 mM) proportion (D).

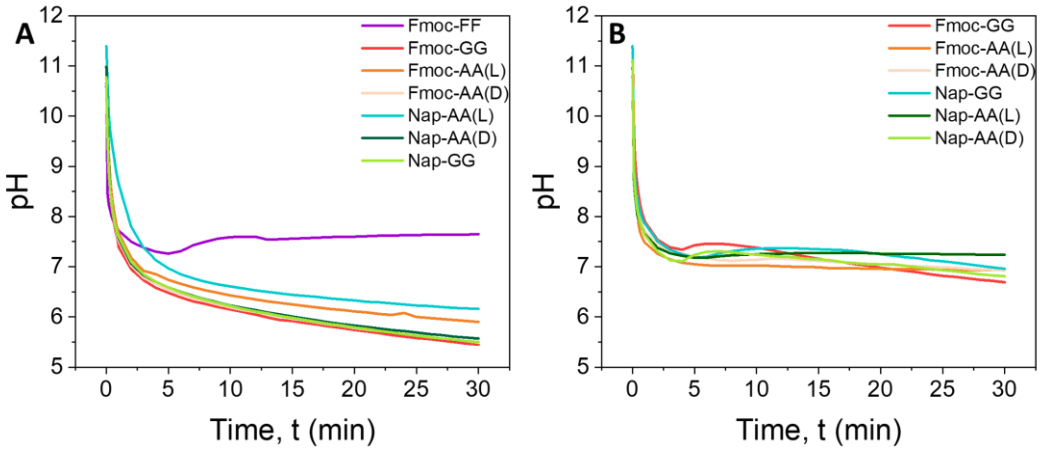

Figure S7. Change in pH versus time of solutions of the dipeptides (final conc. 10 mM at pH 10.6 using NaOH) after de addition of 5 µL of a solution of δ-gluconolactone (200 mg/mL). (A) Change in pH of solutions of individual dipeptides; (B) change in pH of solutions of mixtures of dipeptides Fmoc-FF: other dipeptides at 1:3 ratio.

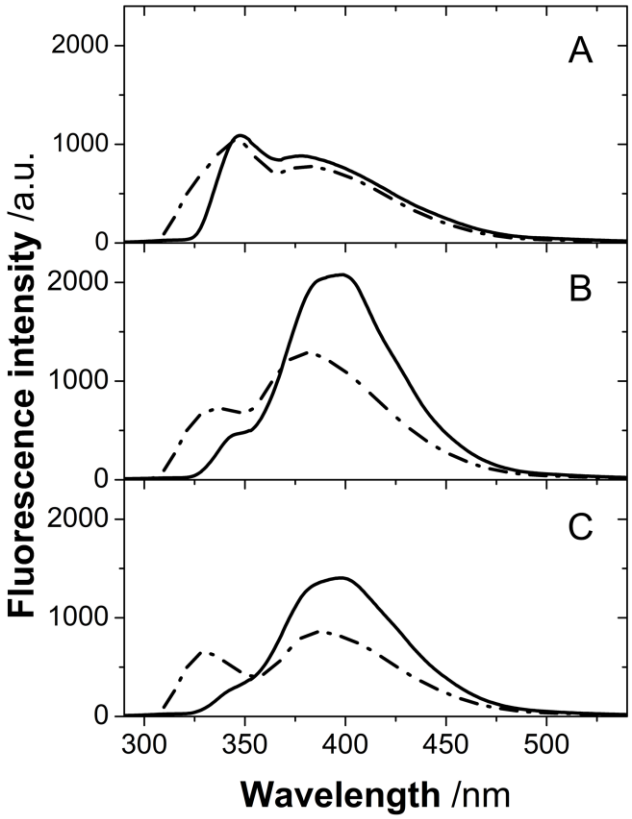

Figure S8. Fluorescence emission spectra (λ_{ex} = 280 nm, solid lines) of 1:3 (2.5 mM: 7.5 mM) ratio mixtures of (A) Fmoc-FF:Nap-AA(L), (B) Fmoc-FF:Nap-AA(D), and (C) Fmoc-FF:Nap-GG. The corresponding simulated spectra in the absence of FRET and other interactions are shown as dash-dotted lines. The simulated spectra were reconstructed by adding up the spectra of the individual peptides (from Figure 6 in main text) at a 1:3 ratio. In a total absence of interaction between the different dipeptides, the experimental and simulated emission spectra should be comparable. Nevertheless, interaction and co-aggregation of Fmoc-FF with Nap-labeled peptide would result in quenching of the Fmoc emission and the subsequent enhancement of the Nap emission.

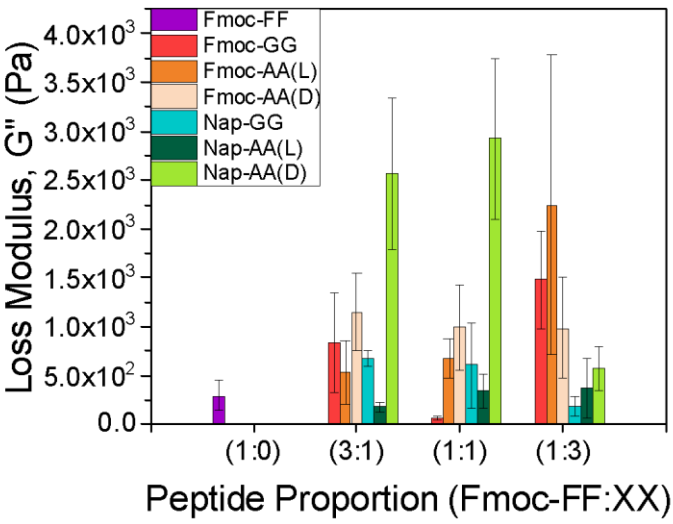

Figure S9. Average loss modulus (G'') in the LVR depending on the dipeptide proportion for hydrogels at a final concentration 10 mM.

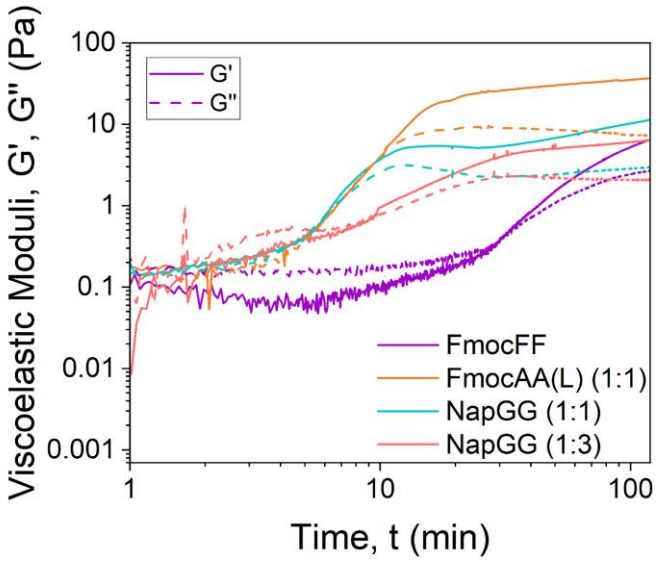

Figure S10. Storage (G') and loss (G'') moduli as a function of time for gelling samples. Measurements started right after addition of δ-gluconolactone at time t = 0. Curves for single Fmoc-FF sample and some Fmoc-FF:other dipeptides mixtures at a total dipeptide concentration of 10 mM are shown. Results for other dipeptides mixtures (not shown here) were similar.

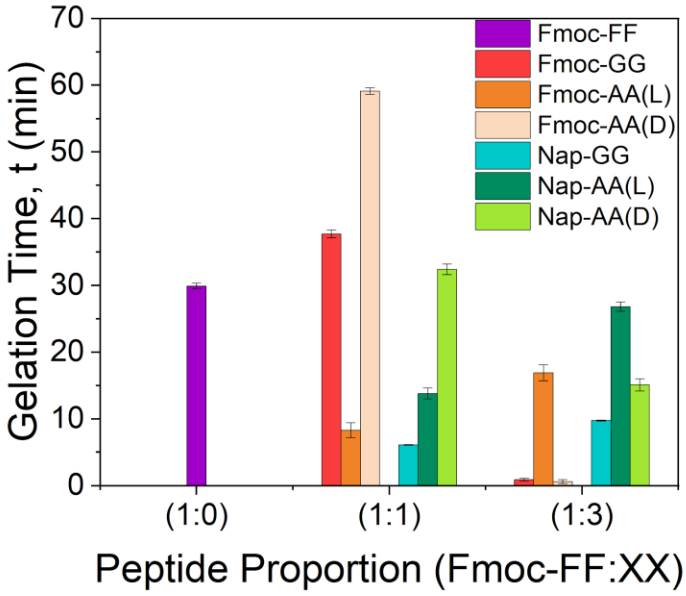

Figure S11. Gelation time for the different dipeptide samples at a final concentration 10 mM. Gelation time is defined as the time for which tanδ crosses a value of 1, in a stable decreasing curve.

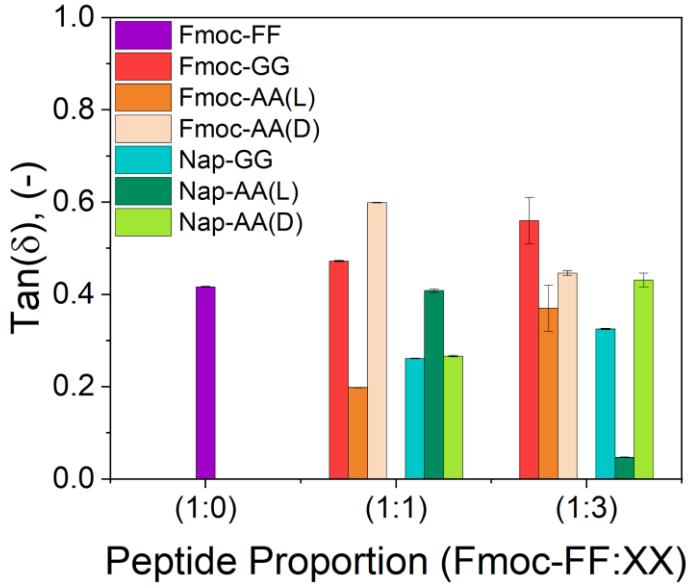

Figure S12. Value of tan δ at time *t* = 120 min after the start of the gelation process for the different dipeptide samples at a final concentration 10 mM.

Table S1. Slope (n) Avrami's equation in sol, transition and gel.

Peptide type	Proportion (Fmoc-FF:XX)	n_{sol}	n_{trans}	n_{gel}
Fmoc-FF	(1:0)	0.10±0.10	5.51±0.17	0.1531±0.0022
Fmoc-Gly-Gly	(1:1)	0.15±0.10	2.63±0.07	1.2227±0.0012
Fmoc-L-Ala-L-Ala	(1:1)	0.64±0.04	3.734±0.009	0.7181±0.0021
	(1:3)	0.47±0.15	1.093±0.015	0.398±0.005
Fmoc-D-Ala-D-Ala	(1:1)	0.45±0.03	2.719±0.013	1.1260±0.0022
Nap-Gly-Gly	(1:1)	1.04±0.03	3.52±0.05	1.193±0.006
	(1:3)	-	1.687±0.011	0.726±0.004
Nap-L-Ala-L-Ala	(1:1)	0.18±0.07	1.847±0.009	0.6240±0.0013
	(1:3)	0.00±0.24	4.94±0.06	0.468±0.013
Nap-D-Ala-D-Ala	(1:3)	0.0±0.3	3.67±0.10	0.3548±0.0006

MOLECULAR DYNAMICS (MD) PROTOCOL

Fmoc-FF, Nap-GG and Fmoc-FF + Nap-GG at 1:1 ratio ensembles were initially constructed using Maestro.[S1] An initial setup of 60 molecules was assembled confronting Fmoc and Naphthyl (Nap) groups on one side and the dipeptide chains on the other in a short of β-sheet packing. The ensembles were next converted to independent pdb files and used for atomistic molecular dynamic (MD) simulation using VMD[S2] and NAMD 2.14.[S3] Fmoc- and Nap-dipeptides were parametrized using LigParGen server[S4-S6] and MD simulation ran using OPLS-AA/M force field.[S7] The initial ensembles were first submitted to a 30 picoseconds (ps) energy minimization at 300K on periodic boundary conditions to remove high-energy contacts, followed by successive 300 ps NVT and a 1 nanosecond (ns) NPT equilibration before the productive 300 ns productive MD simulation. During the productive MD, water bonds were constrained using the SHAKE algorithm;[S8] for every 2 fs, neighbors were searched in grid cells with 1 nm as the cutoff value for short-range neighborlist, electrostatic, and van der Waals; long-range electrostatics were treated with the particle mesh Ewald method[S9] with a grid spacing of 1; constant temperature and pressure were maintained by coupling the system to an external bath at 300 K and 1 bar, using velocity

rescaling[S10] and Parrinello−Rahman,[S11] respectively. A RESPA propagator with the integration time step of 1 fs was used.[S12] TIP3P model was applied for water,[S13] and UCSF Chimera 1.14 was used to perform the trajectory analyses and generate the final images.[S14] The trajectories data were subjected to a RMSD cluster analysis using the MD movie Tool in Chimera setting frame 1 as the starting one, and a step size of 101. The obtained cluster-representative structures were saved as a pdb file and analyzed. Solvent accessible surface area (SASA), H-bonds and rmsd calculations were done using VMD with in-house TLC scripts.

Fmoc-FF AND Nap-GG (1:1) 60 MOLECULES SIMULATION

First, we carried out two 300 ns MD runs of Fmoc-FF and Nap-GG independent ensembles which resulted in different monomers aggregations. The trajectories data were next subjected to a RMSD cluster analysis to obtain the cluster-representative structure of each simulation. The most populated cluster of the Fmoc-FF simulation showed a long rod-like distribution of the monomeric subunits, characterized by Fmoc-Fmoc stacking and H-bonding interactions. The Nap-GG major cluster, however, developed in a more sphere-like distribution of its monomers predominantly controlled by stacking interactions within naphthyl groups (Figure S13).

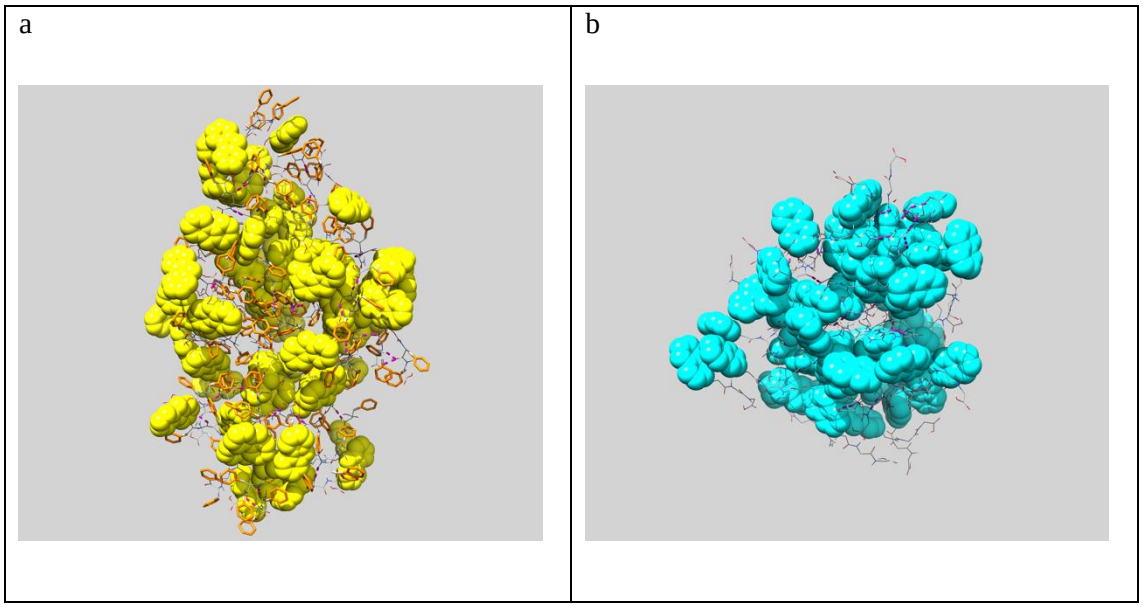

Figure S13. Most representative assembly cluster of Fmoc-FF (a) and Nap-GG (b) (60 molecules) of the 300 ns MD simulations. Fmoc groups and naphthyl groups are represented as yellow and cyan van der Waals spheres, respectively. Diphenylalanine and diglycine peptides are represented

as grey wires and benzyl groups in diphenylalanine as orange sticks. H-bonds are shown as dashed purple lines.

Root-mean-square deviation (RMDS) analysis of the simulated assemblies were carried out to account for the stability of the simulations (Figure S14). For Fmoc-FF, the ensemble remains quite stable for the initial 50 ns changing to an oscillating period in the next 200 ns, and a final stable period at the end of the simulation. On the contrary, Nap-GG ensemble shows a remarkably stable rmsd graph, especially in the first 150 ns of the simulation. These differences could be ascribed to the more dynamic interactions taking place in the Fmoc-FF ensemble dominated by H-bonding interactions, in contrast to the hydrophobic-driven nature in the Nap-GG ensemble.

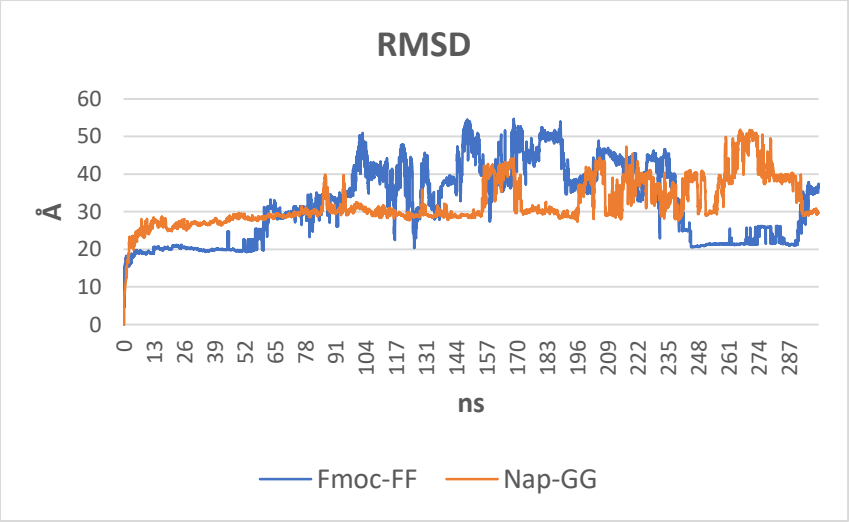

Figure S14. RMSD (Å) for the molecular simulations of Fmoc-FF and Nap-GG monomeric ensembles.

Further analysis of the established H-bonds and solvent accessible surface area (SASA)[S15] of the MD simulations support the cluster distributions discussed above. SASA measurement represent the contact area of the solute (dipeptide monomers in our case) with the solvent, giving information of the changes and rearrangements of hydrophobic surfaces taking place during the simulation. SASA calculations on both, Fmoc-FF and Nap-GG monomeric ensembles, are shown on Figure S15. As seen, the surface exposed area is lower and more stable in the Nap-GG simulation, suggesting a more tightly pack aggregation of this ensemble when compared to the Fmoc-FF one.

These data might explain the sphere-like aggregation of the Nap-GG cluster maximizing the naphthalene's hydrophobic interactions and lowering its solvent exposure.

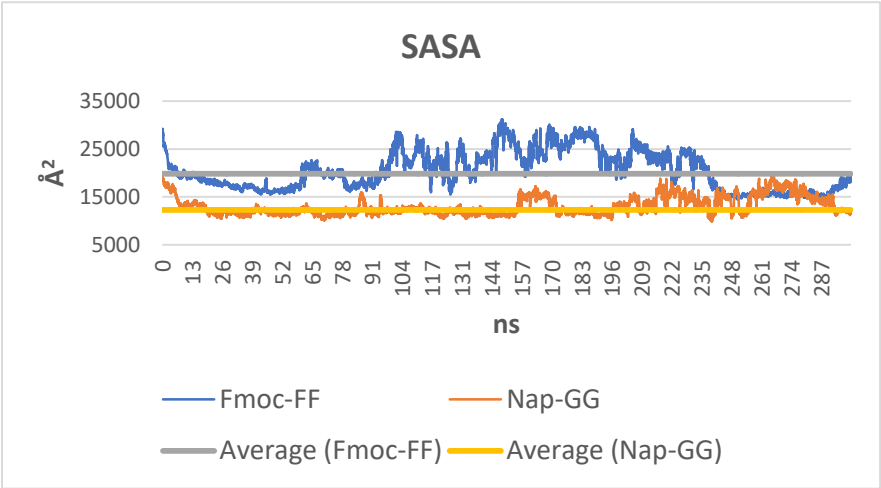

Figure S15. SASA distribution for the 300 ns MD simulations of Fmoc-FF and Nap-GG. Thick horizontal grey and yellow lines correspond to the average solvent-exposed surface in the Fmoc-FF (19818,7 $Å^2$) and Nap-GG (12298,4 $Å^2$) simulations.

On the other hand, analysis of the molecular H-bonds along the whole 300 ns simulations show that the monomeric Fmoc-FF ensemble establish on average 1.8 more H-bonds than the Nap-GG one (Figure S16).

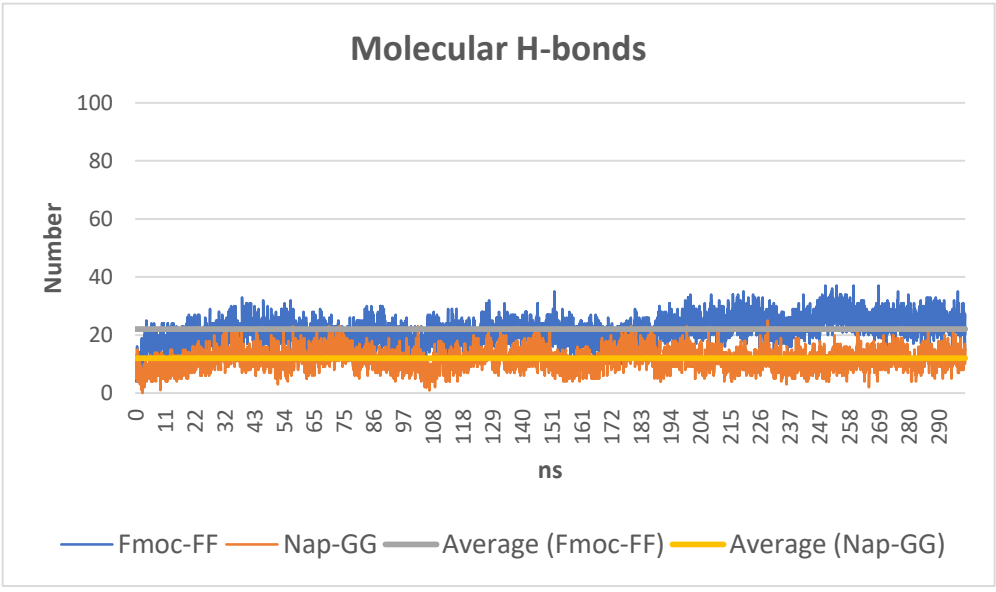

Figure S16. Molecular H-bonds for the 300 ns MD simulations of Fmoc-FF and Nap-GG. Thick horizontal grey and yellow lines correspond to the average number of H-bonds in the Fmoc-FF (22) and Nap-GG (12) simulations.

Next, we simulated ensembles of Fmoc-FF and Nap-GG dipeptides at 1:1 ratio in the same conditions used to simulate the individual monomeric subunits. Hence, ensembles of 60 molecules were constructed and submitted to 300 ns MD simulations and its results analyzed as described above. The major cluster of the Fmoc-FF: Nap-GG ensemble at 1:1 ratio showed a long 2D fibril-like aggregation of interconnected monomeric subunits. The Nap-GG and Fmoc-FF dipeptides appear to display a helical-like arrangement supported by the phenyl rings of Fmoc-FF monomers and a net of H-bonds established within the dipeptides side chains (Figure S17).

<table>
<tr><td>a
 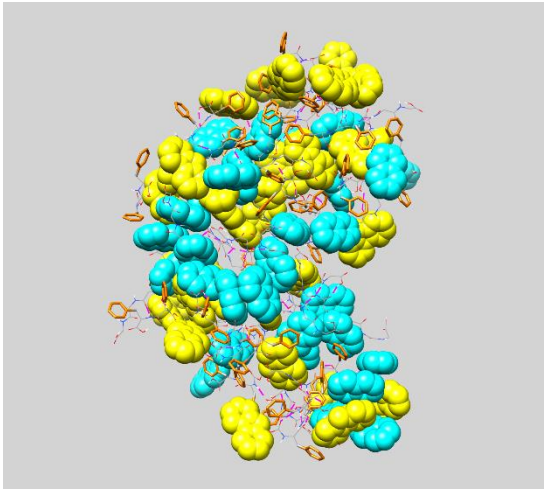 </td><td>b
 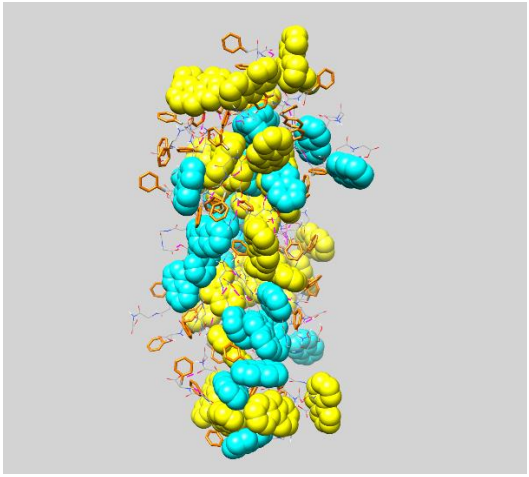 </td></tr>
<tr><td>c</td><td></td></tr>
</table>

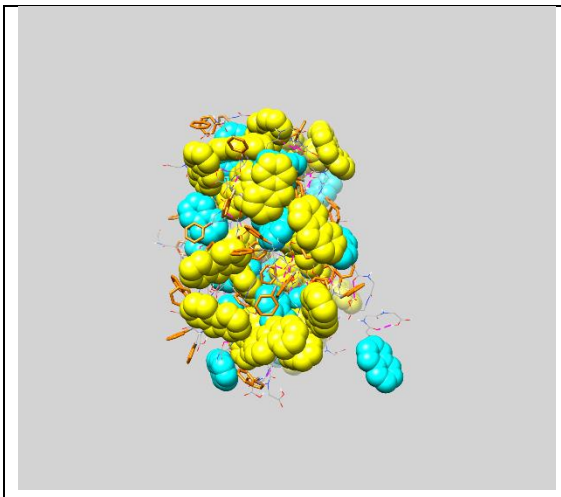

d

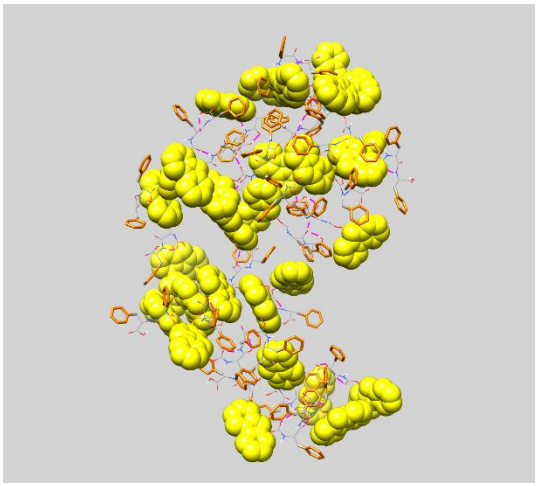

e

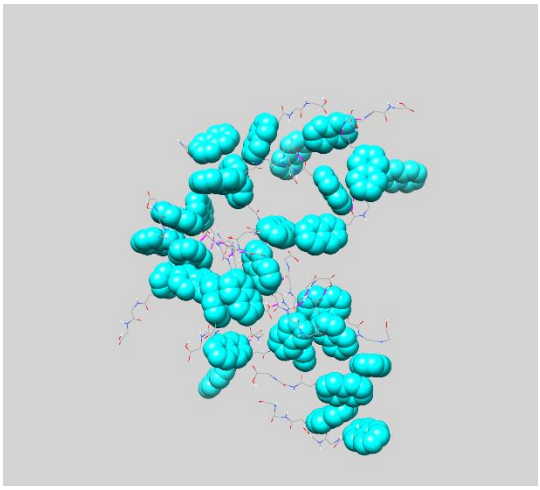

f

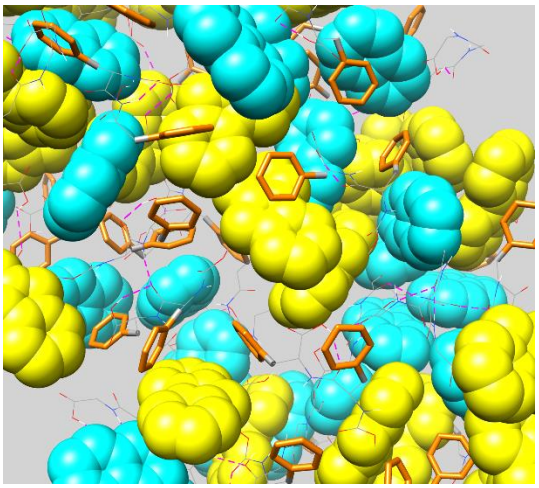

Figure S17. Most representative assembly cluster of Fmoc-FF:Nap-GG (60 molecules, 1:1 ratio) 300 ns MD simulation. Fmoc groups and naphthyl groups are represented as yellow and cyan van der Waals spheres, respectively. Diphenylalanine and diglycine peptides are represented as grey wires. H-bonds are shown as dashed purple lines. (a) Front view; (b) side view; (c) top view; (d) Front view of isolated Fmoc-FF network; (e) Front view of isolated Nap-GG network; (f) Close-up view of the benzyls network (represented as orange sticks) and Fmoc-FF:Nap-GG packings.

On the other hand, RMSD, SASA and molecular H bonds values of the mixture Fmoc-FF:Nap-GG at 1:1 ratio showed intermediate values to the two monomers, which suggests a regular distribution of the two monomers within the fiber as expected for an alternate arrangement (Figues S18, S19 and S20).

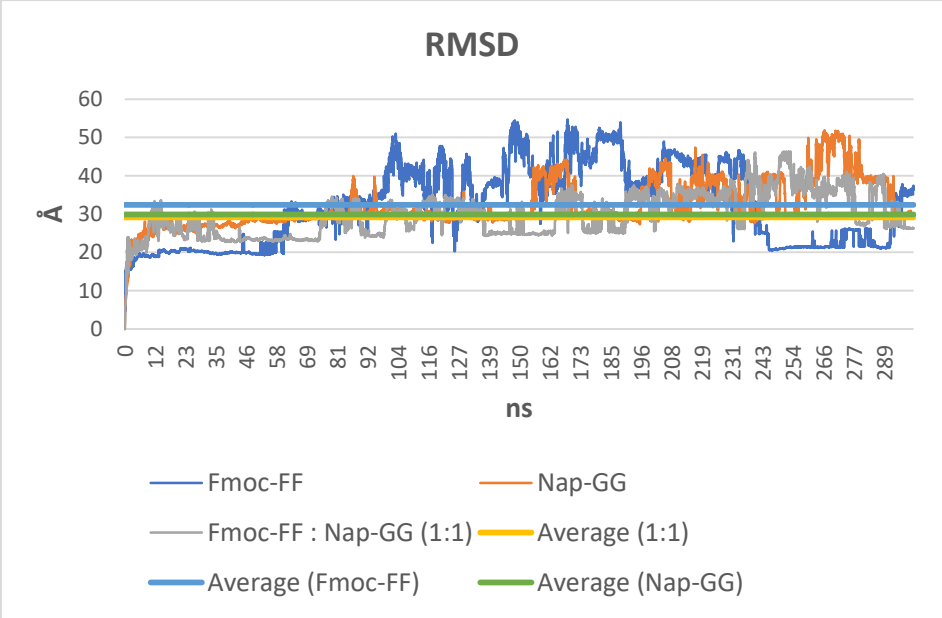

Figure S18. RMSD (Å) for the molecular simulations of Fmoc-FF, Nap-GG monomeric ensembles and Fmoc-FF:Nap-GG at 1:1 ratio.

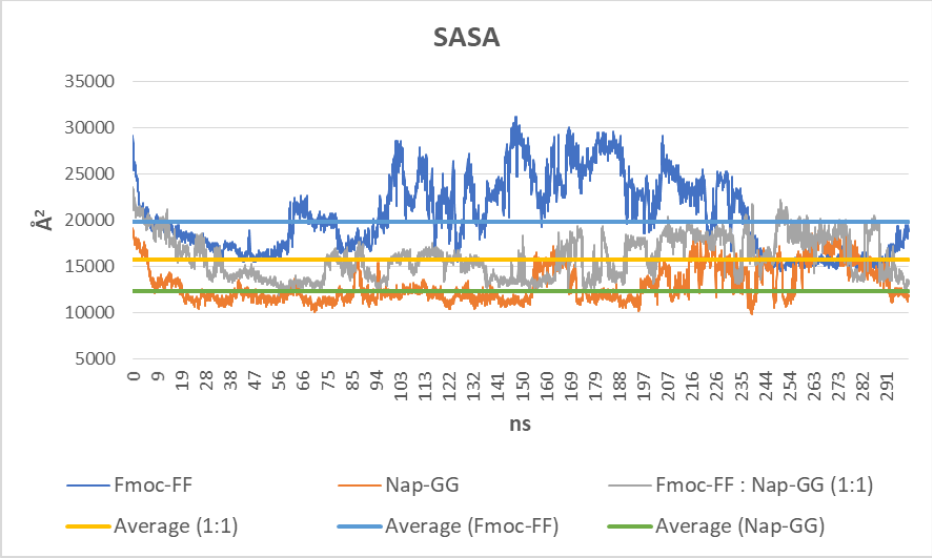

Figure S19. SASA distribution for the 300 ns MD simulations of Fmoc-FF, Nap-GG and Fmoc-FF:Nap-GG at 1:1 ratio. Thick horizontal orange line corresponds to the average solvent-exposed surface in the Fmoc-FF:Nap-GG (15797,5 $Å^2$) simulations.

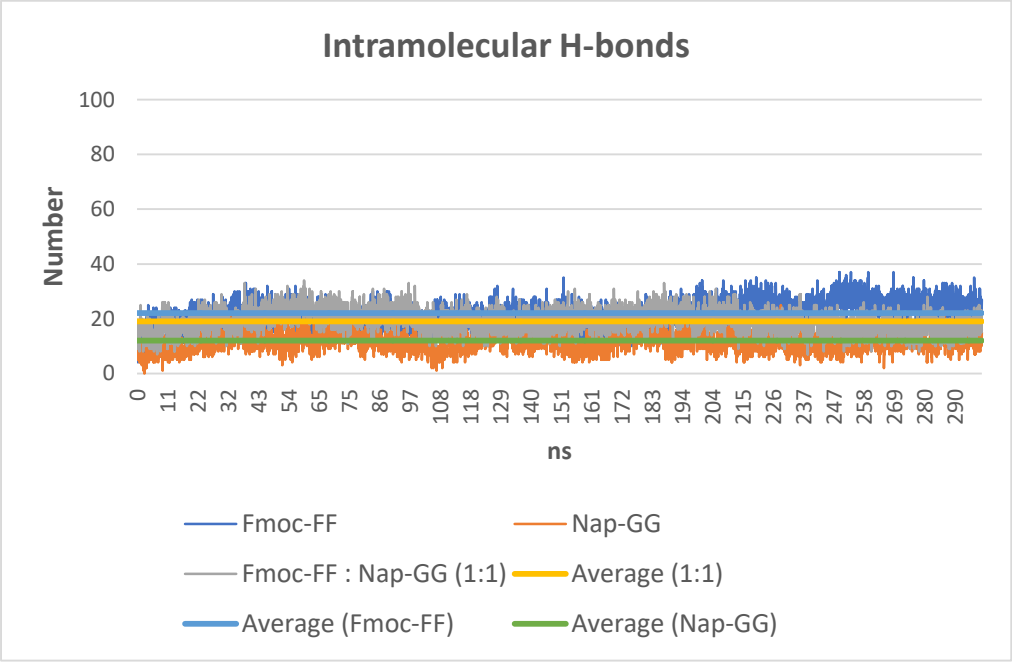

Figure S20. Number of H-bonds for the molecular simulations of Fmoc-FF, Nap-GG and Fmoc-FF:Nap-GG at 1:1 ratio. Thick horizontal orange line corresponds to the average number of H-bonds in the Fmoc-FF:Nap-GG 1:1 (19) simulations.

REFERENCES

S1 Schrödinger Release 2019-1: Maestro, Schrödinger, LLC, New York, NY, 2019.

S2 Humphrey, W.; Dalke, A.; Schulten, K. VMD: Visual Molecular Dynamics. J. Mol. Graphics 1996, **14** (1), 33–38. https://doi.org/10.1016/0263-7855(96)00018-5.

S3 Phillips, J. C.; Hardy, D. J.; Maia, J. D. C.; Stone, J. E.; Ribeiro, J. V.; Bernardi, R. C.; Buch, R.; Fiorin, G.; Hénin, J.; Jiang, W.; McGreevy, R.; Melo, M. C. R.; Radak, B. K.; Skeel, R. D.; Singharoy, A.; Wang, Y.; Roux, B.; Aksimentiev, A.; Luthey-Schulten, Z.; Kalé, L. V.; Schulten, K.; Chipot, C.; Tajkhorshid, E. Scalable Molecular Dynamics on CPU and GPU Architectures with NAMD. J. Chem. Phys. 2020, **153** (4), 044130. https://doi.org/10.1063/5.0014475.

S4 Jorgensen, W. L.; Tirado-Rives, J. Potential Energy Functions for Atomic-Level Simulations of Water and Organic and Biomolecular Systems. Proceedings of the National Academy of Sciences 2005, **102** (19), 6665–6670. https://doi.org/10.1073/pnas.0408037102.

S5 Dodda, L. S.; Cabeza de Vaca, I.; Tirado-Rives, J.; Jorgensen, W. L. LigParGen Web Server: An Automatic OPLS-AA Parameter Generator for Organic Ligands. Nucleic Acids Res 2017, **45** (W1), W331–W336. https://doi.org/10.1093/nar/gkx312.

S6 Dodda, L. S.; Vilseck, J. Z.; Tirado-Rives, J.; Jorgensen, W. L. 1.14*CM1A-LBCC: Localized Bond-Charge Corrected CM1A Charges for Condensed-Phase Simulations. J. Phys. Chem. B 2017, **121** (15), 3864–3870. https://doi.org/10.1021/acs.jpcb.7b00272.

S7 Robertson, M. J.; Tirado-Rives, J.; Jorgensen, W. L. Improved Peptide and Protein Torsional Energetics with the OPLS-AA Force Field. J. Chem. Theory Comput. 2015, **11** (7), 3499–3509. https://doi.org/10.1021/acs.jctc.5b00356.

S8 Ryckaert, J.-P.; Ciccotti, G.; Berendsen, H. J. C. Numerical Integration of the Cartesian Equations of Motion of a System with Constraints: Molecular Dynamics of n-Alkanes. Journal of Computational Physics 1977, **23** (3), 327–341. https://doi.org/10.1016/0021-9991(77)90098-5.

S9 Darden, T.; York, D.; Pedersen, L. Particle Mesh Ewald: An N·log(N) Method for Ewald Sums in Large Systems. J. Chem. Phys. 1993, **98** (12), 10089–10092. https://doi.org/10.1063/1.464397.

S10 Bussi, G.; Donadio, D.; Parrinello, M. Canonical Sampling through Velocity Rescaling. J. Chem. Phys. 2007, **126** (1), 014101. https://doi.org/10.1063/1.2408420.

S11 Parrinello, M.; Rahman, A. Polymorphic Transitions in Single Crystals: A New Molecular Dynamics Method. Journal of Applied Physics 1981, **52** (12), 7182–7190. https://doi.org/10.1063/1.328693.

S12 Tuckerman, M.; Berne, B. J.; Martyna, G. J. Reversible Multiple Time Scale Molecular Dynamics. J. Chem. Phys. 1992, **97** (3), 1990–2001. https://doi.org/10.1063/1.463137.

S13 Jorgensen, W. L.; Chandrasekhar, J.; Madura, J. D.; Impey, R. W.; Klein, M. L. Comparison of Simple Potential Functions for Simulating Liquid Water. J. Chem. Phys. 1983, **79** (2), 926–935. https://doi.org/10.1063/1.445869.

S14 Pettersen, E. F.; Goddard, T. D.; Huang, C. C.; Couch, G. S.; Greenblatt, D. M.; Meng, E. C.; Ferrin, T. E. UCSF Chimera - A Visualization System for Exploratory Research and Analysis. J. Comput. Chem. 2004, **25** (13), 1605–1612. https://doi.org/10.1002/jcc.20084.

S15 Van Lommel, R.; De Borggraeve, W. M.; De Proft, F.; Alonso, M. Computational Tools to Rationalize and Predict the Self-Assembly Behavior of Supramolecular Gels. Gels 2021, **7** (3), 87. https://doi.org/10.3390/gels7030087.